Multifunctional polymeric implant coatings based on gelatin, hyaluronic acid derivative and chain length-controlled poly(arginine)

Helena Knopf-Marques, Julien Barthes, Sarah Lachaal, Angela Mutschler, Céline Muller, Florent Dufour, Morgane Rabineau, Edwin-Joffrey Courtial, Julie Bystroňová, Christophe Marquette, et al.

Version of Record: https://www.sciencedirect.com/science/article/pii/S0928493119311877
Manuscript_96951bbb79f1c8278aabb0fd36cd8bab

MULTIFUNCTIONAL POLYMERIC IMPLANT COATINGS BASED ON GELATIN, HYALURONIC ACID DERIVATIVE AND CHAIN LENGTH-CONTROLLED POLY(ARGININE)

Helena Knopf-Marques[1,2#], Julien Barthes[1,2#], Sarah Lachaal[2], Angela Mutschler[2], Céline Muller[1], Florent Dufour[1], Morgane Rabineau[2,4], Edwin-Joffrey Courtial[5], Julie Bystroňová[6], Christophe Marquette[5], Philippe Lavalle[2,4], Nihal Engin Vrana[1,2]*

[1]Protip Medical, 8 Place de l'Hôpital, 67000 Strasbourg, France

[2]INSERM UMR 1121, 11 rue Humann, 67085 Strasbourg, France

[3]Univ. Bordeaux, CNRS, Bordeaux INP, LCPO, UMR 5629, F-33600, Pessac, France

[4]Université de Strasbourg, Faculté de Chirurgie Dentaire, Fédération de Médecine Translationnelle de Strasbourg, Fédération de Recherche Matériaux et Nanosciences Grand Est, 67000 Strasbourg, France

[5]3dFAB Université Lyon 1 - CNRS 5246 ICBMS, Lyon, France

[6]Contipro Biotech S. R. O., Dolni Dobrouc 401 561 02 Dolni Dobrouc, Czech Republic

Keywords: Multifunctionality, Antimicrobial coatings, ECM, Implants

ABSTRACT

Surface of the implantable devices is the root cause of several complications such as infections, implant loosening and chronic inflammation. There is an urgent need for multifunctional coatings that can address these shortcomings simultaneously in a manner similar to the structures of extracellular matrix. Herein, we developed a coating system composed of ECM components and a naturally derived polypeptide. The interactions between the coating components create an environment that enables incorporation of an antimicrobial/angiogenic polypeptide. The film composition is based gelatin and hyaluronic acid modified with aldehyde groups (HA-Ald) that can react with poly(arginine) (PAR) through transient interactions. Nanoplasmon measurements demonstrated a significantly higher loading of PAR in films containing HA-Ald with longer retention of PAR in the structure. The presence of PAR not only provides to the film surface antimicrobial (contact-killing) properties but also increased endothelial cell-cell contacts (PECAM) and VEGFA gene expression and secretion by human vascular endothelial cells. This multifunctional coating can be easily applied to surface of implants where it can enact on several problems simultaneously.

INTRODUCTION

Foreign body response (FBR) happens upon implantation of a biomaterial in order to protect the body from a foreign object. Reactions of both the implant to the host tissue and of the host on the implantable biomaterial need to be controlled to avoid health complications to the patient and for the stability and long-term functionality of biomaterial. Biomaterial implantation and the associated tissue injury trigger a cascade of inflammatory and wound healing responses that are typical of FBR.[1-3]

Wound healing is a complex process with many factors that can delay healing.[4] Pro-angiogenic and antibacterial effects are both desirable for fast wound healing process after the implantation of a biomaterial into the body. Angiogenesis is a vital process in growth and development: it can be defined as a process by which perfusion pathway length and vessel segment number are increased and organized into a functional vascular bed. In normal situations, this effective increase in vessel density delivers more blood to the tissue, facilitating tissue growth and/or increased tissue activity. Therefore, vascularization is a primary component of tissue growth and repair. In the context of an implanted device, angiogenesis is tightly related to its integration and long-term functionality.[5, 6]

Another important aspect concerning wound healing is associated with the bacterial presence around the implant. Nowadays, about half of hospital-acquired infections (nosocomial infections) are associated to medical devices.[7] Indeed, surfaces of medical devices are an excellent support for bacterial colonization and biofilm formation. The use of antibiotics has low efficiency for these infections because the action of antibiotics inside the biofilms is very limited due the presence of an extracellular matrix-like polymeric structure secreted by bacteria that protects them against external aggression.[8, 9] Moreover, the increase of resistance to antibiotics for

bacterial strains has become a major healthcare problem.[10] Year by year, the number of medical devices used is increasing and the prevalence of infections related to implants reported in the literature is also constantly on the rise. Due to this fact, it has become urgent to protect medical implants against infections.

To prevent bacterial colonization on medical devices, our group developed an antimicrobial coating by using the layer-by-layer technique with poly(arginine) (PAR) as polycation and hyaluronic acid (HA) as polyanion. By controlling the number of arginine residues, an antimicrobial multilayer film was obtained formed with 24 bilayers of PAR30 (30 arginine residues) combined with HA. Thanks to the positive charges of PAR30 that interact with the negatively charged membrane of the bacterial cell, we have proven that this layer-by-layer coating has an antimicrobial effect through contact killing mechanism against several Gram positive and Gram negative bacterial strains and present a good biocompatibility.[11, 12] However, it is yet to be demonstrated that the utilization of PAR30 in conjunction with other coatings can render them antimicrobial.

HA is a glycosaminoglycan that is a good candidate to design biomaterials if it is combined with other extracellular matrix (ECM) components that promotes cell adhesion.[13-15] Furthermore, the mechanical properties of the formed gel can be improved by chemical modification of HA.[14, 16-20] HA also have anti-inflammatory effects in a MW dependent manner.[21, 22] Additionally, HA with high molecular mass can act on endothelial cells, inhibiting proliferation and disrupting monolayers. These effects are significantly dependent on the size of HA present.[23]

To mimic natural microenvironment, we have previously used two ECM components, gelatin type B (denaturated collagen)[24] and hyaluronic acid derivatives, to design a controlled release platform.[25, 26]. To adjust physical parameters of the composite gelatin/HA film, tyramine

conjugated HA was used in order to obtain a crosslinked film: the tyramine conjugated HA is crosslinked by horseradish mediated reaction using horseradish peroxidase (HRP).[25] Moreover, a double crosslinking (an interpenetrating network) is obtained by using the enzyme transglutaminase, which catalyzes the formation of amide crosslink from carboxamide (RCONH2) from glutamine and primary amine functionalities from lysine which are present on gelatin. By these two enzymatic reactions, An interpenetrating network is formed with a better stability.[27] However in this configuration, the crosslinking of HA can only be done between tyraminated groups of HA and the HA derivative could not interact with the added proteins or polysaccharides. With this crosslinking strategy, it is difficult to tune the loading and release properties of the resulting coating.

To design an HA-derivative which can interact transiently with proteins and polysaccharides, hyaluronan-aldehyde was developed aiming to improve protein delivery platform (non-specific interaction with the added components). The process is based on the introduction of short pendant chains of 4-aminobutyraldehyde on the HA backbone.[28] It is known that the aldehyde moieties possess the ability to react with amino compounds under physiological conditions, which makes it advantageous pendant group on the polymeric chain for temporary immobilization of bioactive agents. As most of the growth factors, cytokines and more generally proteins possess amine moieties, they can react and crosslink with such a HA derivative. Another possible type of oxidized HA, is the HA derivative with aldehyde groups in position 6 of the N-acetyl-D-glucosamine part.[29, 30]. One interesting study done by Vanderhooft and colleagues (2009) presented experimental control of both composition and gel stiffness of a semi-synthetic ECM based on cross-linked hyaluronana. As a conclusion, they showed that the mechanical

properties based on rheological studies of the ECM in part determine the ultimate cell phenotype.[31]

In this study, we developed a spin coated, interpenetrating network of gelatin and HA-Aldehyde derivative for controlled release of poly(arginine) (PAR). To improve the stability of the film, gelatin is enzymatically crosslinked with microbial transglutaminase to enable the formation of amide bond within gelatin structure. Then PAR and an HA-Aldehyde derivative can interact i) via formation of ionic pairs where the cations are the protonated guanidinium groups of PAR and the anions are the carboxylic groups of HA, and ii) via formation of a covalent imine bond –CH=N- between aldehyde moieties of HA and amine groups of PAR either on the polymer backbone (guanidinium groups) or on the N-terminal side. The formation of covalent imine bond between PAR and HA is more favorable on the N-terminal side since it is a primary amine with higher reactivity compared to the amine moieties bears by guanidine group which are secondary amines with lower reactivity towards aldehyde. HA-aldehyde and PAR interactions (ionic and covalent) are summarized in Scheme 1.[32] The Gel/HA-Ald film is used as a reservoir of PAR in order to obtain a contact-killing activity over a long period. As a proof of concept, we quantified the effect of the presence of PAR in the coating on its antibacterial and endothelial cell behavior. Arginine is an important component in both metabolism of macrophages[33] (as its conversion by arginase is implicated in anti-inflammatory macrophage phenotype development) and vascular endothelial cells (as it is the source material for nitric oxide synthesis, a potent angiogenic molecule).[34] Thus incorporation of an arginine source in the form of a polypeptide can contribute to the triggering of angiogenesis and anti-inflammatory polarization of macrophages.[35] In this work we have used the Nanoplasmonic Sensing (NPS) developed by Insploriom for quantifying the PAR adsorbed on the gelatin samples surface. NPS is a versatile

surface sensitive optical technique for studies of properties in molecular scale films, using leading nanoparticles, often gold or silver, as local sensing elements.

As a highly strong polycation, we have already demonstrated the antimicrobial and anti-inflammatory properties of poly(arginine)[36] and ECM based coatings has been shown to have beneficial immunomodulatory properties.[37] Thus we hypothesized that its incorporation together with a derivative of a known immunomodulatory and angiogenic biomacromolecule (HA) can significantly improve the capacities of polymer based, multifunctional, implant coatings.

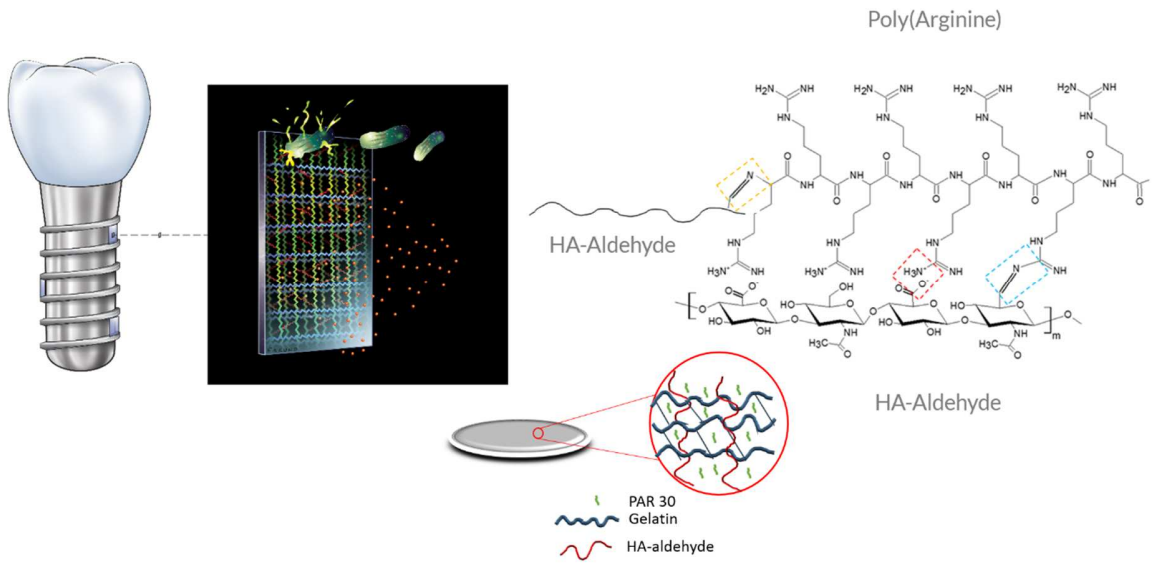

Scheme 1. A multifunctional coating system composed of ECM components that can be attached to implants (such as dental prosthesis) and other biomedical devices, to prevent peri-implantitis and to improve angiogenesis responses. All the possible interactions between PAR and HA-Aldehyde are illustrated in different colors; i) red dashes represent ionic interactions between cations on PAR chains (protonated guanidinium groups) and the anions on HA (carboxylic group), ii) yellows dashes represent the formation of imine bond between primary amine on PAR

N-terminal side and aldehyde group on HA and iii) blues dashes represent the formation of imine bond between the guanidine group on PAR backbone and aldehyde group on HA.

EXPERIMENTAL SECTION

Material Preparation

Gelatin type B (Mw =2-2.5×10^4 Da, pI = 4.7-5.2) from bovine skin, fluorescein isothiocyanate labeled bovine serum albumine (BSA-FITC, Mw = 6.6×10^4 Da) were purchased from Sigma Aldrich (St. Quentin Fallavier, France). Microbial Transglutaminase (TGA) (Mw =3.8×10^4 Da, pI = 9) was kindly provided by Ajinomoto (Japan). HA-Aldehyde (HA-Ald, Mw = 4.36 x 10^5 Da) was provided by CONTIPRO (Dolni Dobrouc, Czech Republic). Poly(arginine hydrochloride) with 30 arginine residues (PAR30, Mw = 6.4 x 10^3 Da) was purchased from Alamanda Polymers (USA).

Gelatin (Gel) and Gelatin/Hyaluronic Acid – Aldehyde derivative (Gel/HA-Ald) films were obtained by spin coating (WS-650Mz-23NPP from Laurell, North Wales, US). The films were prepared by dissolution of adequate amounts powders of Gelatin (5% or 4.5% w/v for Gel or Gel/HA-Ald, respectively) mixed with HA-Aldehyde (0.5% w/v) in 0.15 M NaCl/10 mM Tris solutions (pH = 7.4). The solution was heated to 50°C with constant stirring. Then 200 µL of this hot solution were placed on a glass slide with 12mm of diameter and the spin coating was carried out with the following parameters: 2500 rpm with an acceleration of 1250 rpm, for 2 minutes. The films were then kept dry at 4°C for at least 3 hours before use. All solutions were prepared using ultrapure water (Milli Q-plus system, Millipore) with a resistivity of 18.2 MΩ.cm. As a final step, the films were crosslinked with transglutaminase enzyme (10% w/v) in PBS at room temperature for 30 minutes.

Fluorescent Labeling of PAR. For labeling PAR chains, PAR (156 nmol in 100 mM $NaHCO_3$ pH 8.3 buffer) was incubated with fluorescein isothiocyanate (FITC, Sigma-Aldrich, France) at a 1:2 molar ratio of PAR/FITC at room temperature for 3 h. This solution was dialyzed against 1 L of water at 4 °C with a Slide-A-Lyser Dialysis Cassette (Thermo-Fisher Scientific Inc., USA), cutoff = 3500 MWCO. PAR-FITC was then produced and stored in aliquots of 2 mL (78 nmol in NaCl-TRIS buffer).

Gel and Gel/HA-Ald films charged with PAR

The following conditions were used for PAR supplementation: Gel and Gel/HA-Ald films in presence of absence of PAR. The PAR (50 µL at 30µM) was first incubated on the top of the films overnight at 4°C and let dry the next day prior to perform the experiment described in the next steps.

Material Characterization

Degradation of Gel and Gel/HA-Ald was performed at 37°C for 3 days by incubating the films in PBS (2 mL). These films were analyzed using the "Sirius Red/Fast Green Collagen Staining Kit" (Chondrex, Redmond, US) to determine the amounts of collagen (thus gelatin). Sirius Red (OD 540 nm) specifically binds collagens or collagen derived structures such as Gelatin and is used for detecting all types and species of collagen, whereas Fast Green (OD 605 nm) binds to non-collagenous proteins. To perform the analysis, dye solution (0.2 mL) was added on the film and incubated at room temperature for 30 min. Then, the dye solution was removed, and the film was rinsed with distilled water. Finally, dye extraction solution (1 mL) was added to the film to dissolve the film and quantify the dye. Then, the OD was read at 540 nm and 605 nm and the following equation was used as described in the protocol given by the manufacturer:

$$\text{Gelatin } (\mu g/\text{sample}) = (OD_{540} - (OD_{605} \times 0.291))/0.0378.$$

These results were compared to those obtained with non-degraded dry Gel or Gel/HA-Ald films.

The poly(arginine) (PAR) adsorption on Gel and Gel/HA-Ald was studied using the nanoplasmonic sensing (NPS, Insplorion Xnano, Gothenburg, Sweden) (for details please see supplementary information). The Xnano consists of a flow chamber to which analytes are delivered via a peristaltic pump, and an optical analysis unit. The adsorption was measured in real-time using NPS. NPS is based on the physical phenomenon of localized surface plasmon resonance, LSPR. The sensors consist of glass slides with gold nanodisks attached to the surface. The plasmonic resonance in the disks were excited using white light and the optical spectra was then analysed using a spectrophotometer and the software Insplorer. In real-time, the spectral plasmonic peak position was calculated. The response of an NPS sensor is given by the equation:

(Eq1) $\Delta\lambda_{NPS} = S_0 \cdot \Delta n_a$, wherein S0 is the sensor sensitivity expressed in nm/RIU (refractive index unit) and Δna is the change in ambient refractive index.

When the sample is significantly thicker than the NPS probe depth and under the assumption that the sample is uniform and that the refractive index increment (dns/dc) for the sample is known, the volume mass concentration for the sample (cs) can be determined:

(Eq. 2) $$c_s = \frac{\Delta n_s}{dn_s/dc} = \frac{\Delta\lambda_{NPS}}{S_0 \cdot dn_s/dc}$$

The details of the equations and the methodology is given in supplementary (Note S1).

A baseline was obtained in PBS and results are displayed as shift from this baseline, ΔλNPS peak (nm). Briefly, sensors were spin coated with Gel and Gel/HA-Ald, and then those films were crosslinked before going into the measurement chamber. The sensors with the films were put into the flow chamber and the PAR solution (78nmol in PBS) was flowed over at a rate of

100 µL.min^{-1}. In real-time, the centroid of the plasmonic resonance is measured. Using equation 2, we were able to determine mass concentration for each sample.

The PAR release from the films was monitored with a Genius XC spectrofluorimeter (SAFAS, Monaco). PAR-FITC (50 µL at 78nmol) (see section Fluorescent Labeling of PAR) was previously incubated on the top of the films overnight at 4°C and let dry the next day prior to perform release experiment. The release experiment was carried out at 37°C in PBS (350 µL of PBS per sample). Fresh PBS solution was added after each supernatant collection. The supernatants were analyzed with the spectrofluorimeter. The wavelengths of excitation and emission for FITC are $\lambda_{ex}/\lambda_{em}$ = 495 nm/520 nm. After each analysis, a new PBS solution was added and then a cumulative release was calculated.

A rotational rheometer (AR 2000, TA Instruments, New Castle, US) was used to characterize viscoelastic behaviors of the films with parallel-plate geometry (40 mm) using insulated solvent trap to provide effective inhibition of solvent loss. Characterization was performed in dynamic mode (1 rad/s) through time sweep procedure at 37°C (controlled by a Peltier plate steel).

Cell culture

For cell experiments in 2D (cells seeded on top of the film), the study was performed with HUVECs (Human Umbilical Vein Endothelial cells, PromoCell, Heidelberg, Germany) and Human Fibroblasts (BJ foreskin fibroblasts, ATCC, Manassas, US).

The HUVEC cells were used at passages between 4 and 8. The culture media used were endothelial cell growth medium (PromoCell) for HUVECs. The supplement used for these cells were Supplement Mix C-39215 (containing hydrocortisone, heparin, fetal calf serum, basic fibroblast growth factor, epithelial growth factor and endothelial cell growth supplement). Cells, in a 75 cm2 flask, were first cultivated to a near-confluent state. Then, cells were trypsinized

using Detachkit from Promocell. Before seeding cells, Gel/HA-Ald films were UV treated for 15 min. For each cell experiment 50 000 cells were deposited on top of Gelatin and Gelatin/HA films in a 24-well plate that was first incubated for 15 min at 37°C for adhesion and then media (1 mL) were added. The plate was then incubated at 37°C.

The metabolic activity of cells seeded on Gel or Gel/HA-Ald films was measured with the in vitro Toxicology Assay Kit (a resazurin based test) (Sigma Aldrich). This test is based on the reduction of resazurin dye which will become fluorescent (red) when incubated with viable cells. 500 µL of resazurin solution (10% v/v) in culture medium were deposited in each well plate and maintained 2 h in incubator. Then the solution was read with the spectrofluorimeter (λ_{ex}/ λ_{em} = 560 nm / 590 nm).

Real-time RT-qPCR

Real-time reverse transcription qPCR (real-time RT-qPCR) was used for quantifying biologically relevant changes in expression levels of selected genes for HUVEC cells seeded on coatings. The levels of vascular endothelial growth factor A (VEGFA) gene expression related to angiogenesis, were measured by Real time qPCR using 96-well Prime PCR custom plate (Bio-Rad, Hercules, California, US). Reactions were carried out for 50 cycles in a CFX-Connect (Bio-Rad). HPRT1 (Hypoxanthine Phosphoribosyltransferase 1) and RPS18 (Ribosomal Protein S18) were used as reference gene after a screening for the most suitable housekeeping gene for all the RT-qPCR obtained results.

Antibacterial Assay

Staphylococcus aureus (*S. aureus*, ATCC 25923) strain was used to assess the antibacterial properties of the samples. Bacterial strain was cultured aerobically at 37 °C in Mueller Hinton Broth (MHB) (Merck, Darmstadt Germany), pH 7.4. One colony was transferred to 10 mL of

MHB medium and incubated at 37 °C for 20 h to obtain bacteria in the mid logarithmic phase of growth. The OD at 620 nm (A_{620}) of overnight culture was adjusted to 0.001, corresponding to a final density of 8.105 CFU·mL^{-1}. Gel and Gel/HA-Ald films are sterilized by using UV-light during 15 min and then washed with sterilized buffer containing 150 mM NaCl and 10 mM of TRIS (Tris(hydroxymethyl)-aminomethane, Merck) at pH 7.4 (denoted NaCl-TRIS buffer).

After washing, each glass slide was deposited in 24-well plates with 300 µL of *S. aureus*, with absorbance adjusted to A_{620} = 0.001, and incubated during 24 h at 37 °C. For negative control, uncoated glass slides were directly incubated with S. aureus using a similar method. For positive control, tetracycline (10 µg·mL^{-1}) and cefotaxime (0.1 µg·mL^{-1}) were added in the *S. aureus* solution that was in contact with uncoated glass slides. To quantify bacteria growth or inhibition after 24 h, the absorbance of the supernatant at 620 nm was measured and the Normalized Pathogen Growth (NPG) of the sample was calculated according to this equation:

(Eq. 3) $$NPG\ (\%) = \left(\frac{A_{620}\ sample - A_{620}\ positive\ control}{A_{620}\ negative\ controle - A_{620}\ positive\ control}\right) \times 100$$

Microscopy characterization

To check the viability of cells, Apoptotic/Necrotic/Healthy Cells Detection Kit from Promokine (PromoCell) was used to quantify apoptotic (green fluorescence for FITC-Annexin labelling of apoptotic cells), necrotic (red fluorescence for Ethidium homodimer III) and healthy cells (blue fluorescence for Hoechst) with a fluorescent microscope. Films with cells were rinsed several times with PBS. Then 100 µL of staining solution (5 µL of each dye for 100 µL of binding buffer provided by the kit) was incubated for 15 min at room temperature and after

several rinsing steps, the films were visualized with a fluorescent microscope (Nikon Eclipse TI-S, Japan).

For morphological characterization of HUVECs, cells were then incubated in a Triton X-solution (0.1% in PBS) for 5 minutes for permeabilisation. Then two rinsing steps with PBS were performed and the samples were incubated for 20 minutes with BSA solution (1% v/v) in PBS. DAPI/Phalloidin staining and PECAM-1 (CD31, cell-cell contact related cell membrane protein, a marker of endothelial barrier formation) immunofluorescent staining were performed. After fixation with 4% paraformaldehyde (for 5 minutes), samples were incubated for 90 minutes with primary antibody PECAM-1 (CD31) (Mab mouse anti-human, [0.938 mg/mL], Thermo Scientific) at a dilution of 1/150 in PBS. Then these samples were incubated for 30 minutes with secondary antibody (Goat anti-mouse IgG, Oregon green 488 conjugate, [2mg.mL-1], Thermo Scientific) at a dilution of 1/200 in PBS and two rinsing steps with PBS were performed. Then, samples were incubated for 1 hour with fluorescent dye conjugated Phalloidin (Alexa Fluor 568 Phalloidin, [6.6 µM], Molecular Probes Life Technologies) at a dilution of 1/40 in BSA solution (1% v/v in PBS) and two more rinsing steps with PBS were performed. The labeled cells were analyzed with confocal laser scanning microscope (Zeiss LSM 710, Germany), and with fluorescent microscope (Nikon Eclipse TI-S, Japan).

Time-Lapse Microscopy

Gelatin and Gelatin/HA-Ald films were sterilized by using UV-light for 15 min and then washed with NaCl-TRIS buffer. After washing, each glass slide was mounted in a Ludin Chamber (Life Imaging Services, Switzerland) with 800 µL of S. aureus (A620 = 4.10-4) in MHB. The time-lapse sequence was performed during 24 h with a Nikon TIE microscope equipped with a 60 × PL APO oil (1.4 NA) objective and an Andor Zyla sCMOS camera (Andor

Technology LtD. United Kingdom). Nikon NIS-Elements Ar software (Nikon, France) was used to image and Phase contrast and fluorescence images were acquired every 5 min for 24 h. Images were processed with ImageJ.

Statistics

The statistical significance of the obtained data was assessed using the t-test, ($n \geq 3$). The error bars are representative of Standard Deviation (SD). For any given experiment, each data point represents the mean ± standard deviation of three replicates. Differences at $p \geq 0.05$ were considered statistically not significant.

RESULTS AND DISCUSSION

Physical and mechanical characterizations of gelatin based coatings

To study the interaction of HA-aldehyde with poly(arginine) (PAR), we have first studied the loading capacity of three different coatings, Gelatin type B (Gel), Gelatin type B / native HA (Gel/HA) and Gelatin type B / HA-Aldehyde (Gel/HA-Ald). PAR adsorption on Gel, Gel/HA and Gelatin/HA-Ald films was studied with the NanoPlasmonic Sensing (NPS) (Figure 1A). To do that, coatings built on sensors were put in a flow chamber and the PAR solution (78 $nmol.mL^{-1}$ in PBS) was flowed over at a rate of 100 $\mu L.min^{-1}$ and the plasmonic resonance was measured until a plateau was reached. At this point, using equation 2 described in experimental section, we were able to determine the concentration of PAR in the coating. The PAR adsorbed on the coating was much higher for Gel/HA-Ald (25$nmol.mL^{-1-}$ than for Gel (6 $nmol.mL^{-1}$) and Gel/HA (5 $nmol.mL^{-1}$), as the Δ?? is proportional to adsorbed molecules on the surface. The addition of native HA in the film formulation did not have beneficial effect on the loading capacity since the results were not statistically significant. However, the presence of HA-aldehyde increases

significantly the quantity of PAR loaded in the film. This can be explained by interactions between the PAR and the HA-Aldehyde derivative via formation of a covalent imine bond –CH=N- between aldehyde moieties of HA and terminal amino groups of PAR or amino groups on guanidine group present on PAR backbone. Based on these results, the beneficial effect of having HA-Aldehyde instead of native HA in the film formulation was demonstrated and for the rest of the study Gelatin and Gelatin/HA-Aldehyde films were used.

Then release experiments of fluorescently labeled PAR (PAR-FITC) were performed in PBS solution and the data were monitored every day until 7 days. A burst release was observed for both cases but this burst release was higher in the case of Gel film (Figure 1B). Hence, the films containing HA-Ald are more prone to keeping the PAR within their structure which can result in longer contact killing capacity. The burst release mostly attributed to the release of molecules only adsorbed on the surface can be explained by the lack of interaction between PAR and the coating and Gel film as previously explained in Figure 1A. Then a steady release for both cases was observed until day 7 mostly attributed to the diffusion of the PAR out of the coating.

Through these experiments, we have observed a higher loading capacity of PAR for the Gel/HA-Ald film but a lowest release profile meaning that the formation of a covalent imine bond between aldehyde moieties of HA and amino groups of the PAR enable the coating to act as a retentive substrate for PAR. The details of the release are given in Table S1.

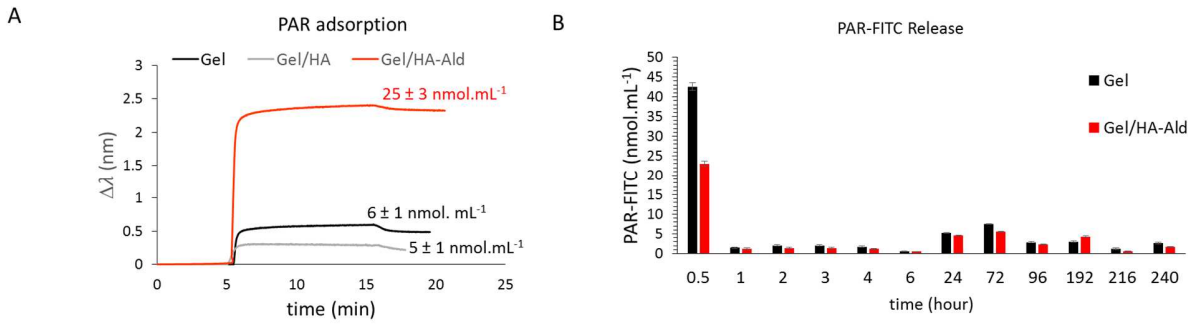

Figure 1. (A) PAR adsorption study on Gel, Gel/HA and Gel/HA-Ald using NanoPlasmonic Sensing (NPS). (B) Kinetic of PAR release from Gel and Gel/HA-Ald in PBS at 37°C, the PAR was deposited on the sample and dried before the experiments release. Experiments were performed with 3 different samples.

The advantage of Gel/HA-Ald film is that we are able to load more of a contact killing antimicrobial agent (hence a longer activity) while keeping it in place for a longer period of time also. On figure 1A it was demonstrated that Gel/HA-Ald films have higher loading capacity than Gel films (>4 times more: from 6 to 25 nmol/mL). However, the release experiments have shown that Gelatin films exhibit higher burst release profile the first day (almost 2 times more: from 23 to 43 nmol/mL) than Gel/HA-Ald and then the release profile between these two coatings was equivalent overtime until day 10. From these experiments, we can then conclude that Gel-HA-Ald films act as a better reservoir for PAR and the retention of PAR within the coating structure especially the first day of release experiment can be explained by the formation of covalent imine bond formation between aldehyde moieties of HA and amino group of PAR.

Then we checked if the addition of HA-Ald in the film changed the overall film stability and mechanical properties of the gelatin-based coating. In Figure S1A, we have quantified the remaining gelatin in the film after 7 days of incubation in PBS solution at 37°C and we have found higher percentage of gelatin in the case of Gel/HA-Ald coating (around 80%) compare to Gel film (around 65%). We can conclude that the addition of HA-Ald in enzymatically crosslinked network improved the overall film stability.

As others studies [38], rheological tests were also performed in order to obtain more information about the viscoelastic properties of the films (Figure S1B). Gel and Gel/HA-Ald films converge to the same viscoelastic behaviors after crosslinking reaction. However, elastic part (G') of

Gel/HA-Ald film is greater than Gel film at the beginning of crosslinking reaction (< 20 min). Moreover, gelation point (G'=G") of Gel/HA-Ald film seems to be immediate (< 4 min) whereas for Gel alone it is obtained at 30 min, which gives an advantage to the composite system in in-situ applications. Indeed, the increase of rheological properties can provided some capabilities in industrial processes, such as coating or 3d printing, with an adequate viscosity, yield stress and a low thixotropic characters.[39-41]

Biological characterization

In order to evaluate the biocompatibility of PAR in the films, different concentrations of PAR were incubated on top of the films composed of 5% gelatin. Then, fibroblasts were seeded on films and incubated for 24 h at 37° C. After 24 hours, metabolic activity was evaluated. In this study and according to ISO Standard 10993-5, the concentration of PAR that allows to maintain the viability of fibroblasts of about at least 70% will be used for the rest of the study. Finally, PAR incubated on the films was considered as non-toxic for quantities equal or below 1.5 nmol (Figure 2A). To study angiogenic and antibacterial properties of the coatings, 1.5 nmol, was thus incubated on the films.

Endothelial cell behavior

To study cell behavior once seeded on Gel/HA-Ald only or charged with 1.5 nmol of PAR, we have used vascular endothelial cells which are the primary constituents of capillaries and blood vessels. The metabolic activity, viability and the cellular morphology has been checked through F-Actin/Nucleus stainings of HUVECs cultivated either on Gel or Gel/HA-Ald films with and without PAR supplementation. We have also checked a marker more relevant for angiogenesis, PECAM-1 CD 31. PECAM-1 CD 31 is a membrane protein expressed on the surface of

endothelial cells. It is a marker of endothelial intercellular junctions present at the early stages of angiogenesis.[42, 43] The analysis of the metabolic activity of HUVECs on the coatings shown an increase over time which was independent of film formulation (Figure 2B). Presence of PAR did not modify the metabolic activity. The morphology of those cells through F-Actin and nucleus stainings was also analyzed by confocal microscopy, as shown in Figure 2 C-F. After 7 days of culture, the cells are uniformly distributed and spread on all the films. Moreover, the viability test done after 1, 3 and 7 days of culture, shows that about 90% of HUVEC cells were viable when seeded on Gel and Gel/HA-Ald with or without PAR. These results show that the supplementation with PAR did not modify HUVEC viability on these coatings. Moreover, the presence of HA-Ald did not alter the metabolism and viability of HUVECs.

Moreover, we have shown the cell-cell contact (intercellular junctions) by confocal images, Figure 3. Comparing Fig. 3 A with B, we can see that the cell-cell contact is higher once the gelatin film is charged with PAR. Furthermore, the same trend was also observed with Gel/HA-Ald coating. There is no significant difference in this aspect between Gel and Gel/HA-Ald films in this aspect. But this stems from the fact that the angiogenic properties are due to PAR and not from the film formulation. The film formulation is conceived for controlling antimicrobial activities. In general, a better defined endothelial cell-cell junctions were seen after the addition of PAR within the structure (Figure 3C-D). Regarding Figure 4, it was shown that the expression of Vascular endothelial growth factor A (VEGFA) characterized by qPCR was more important for the coatings supplemented with PAR regardless of the film composition. Based on these results with PECAM CD31 staining and RT-qPCR readouts, the endothelial cell-cell contacts can probably be attributed to PAR supplementation within the film. Even if the cellular junctions were slightly better defined with HA-Ald, the most distinctive effect was due to PAR presence.

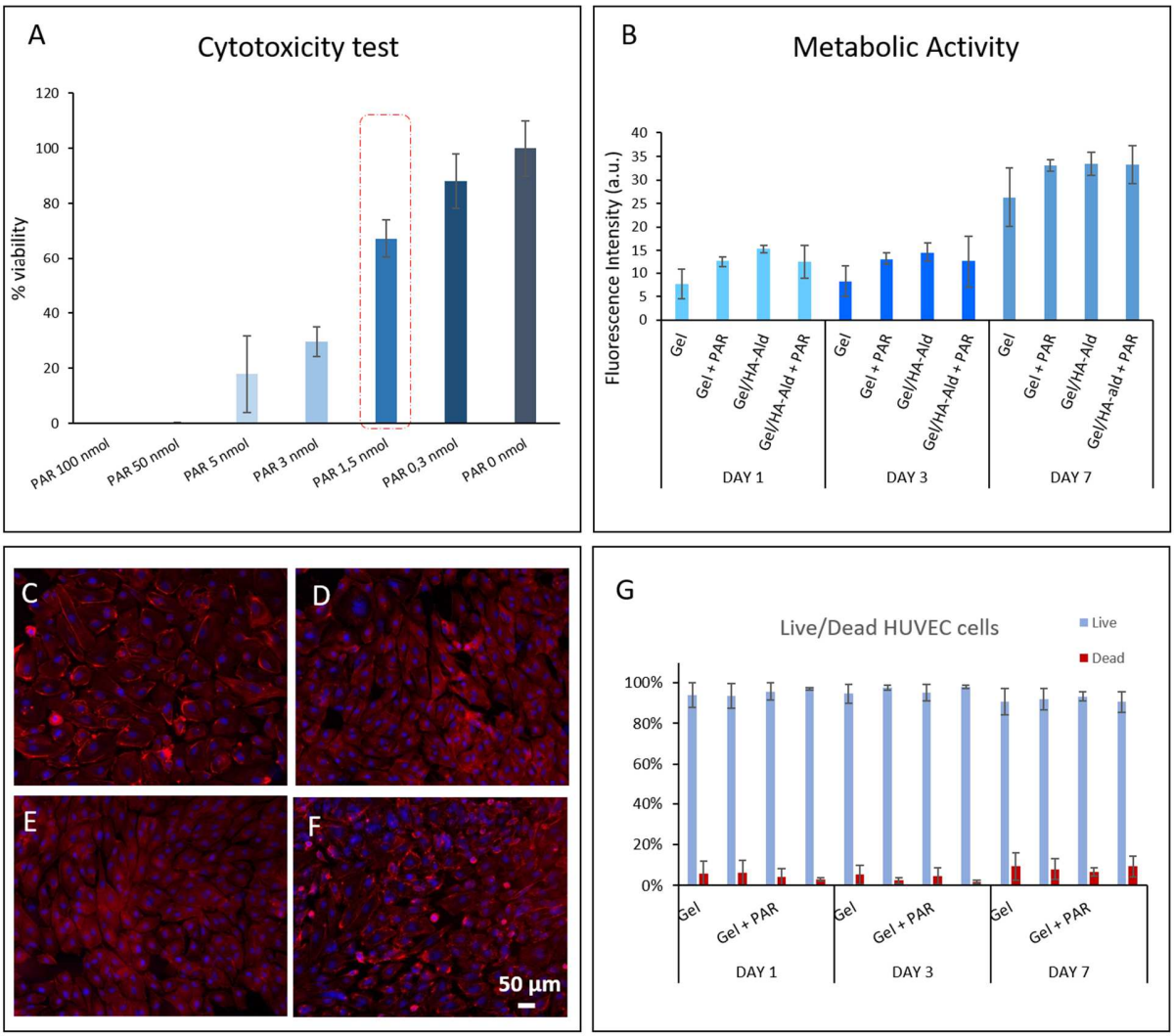

Figure 2. Cytotoxicity test of PAR incubated on gelatin films (A), obtained by alamar blue test. Metabolic activity of HUVEC cells seeded on Gel, Gel+PAR, Gel/HA-Ald and Gel/HA-Ald+PAR as a function of time (B), alamar blue test. Images of HUVEC cells seeded on Gel (C), Gel+PAR (D), Gel/HA-Ald (E) and Gel/HA-Ald+PAR (F) after 7 days of culture. F-actin was stained with Alexa Flour 568 phalloidin and nuclear DNA with DAPI (blue). Live and Dead test for HUVEC cells seed on gelatin films (G).

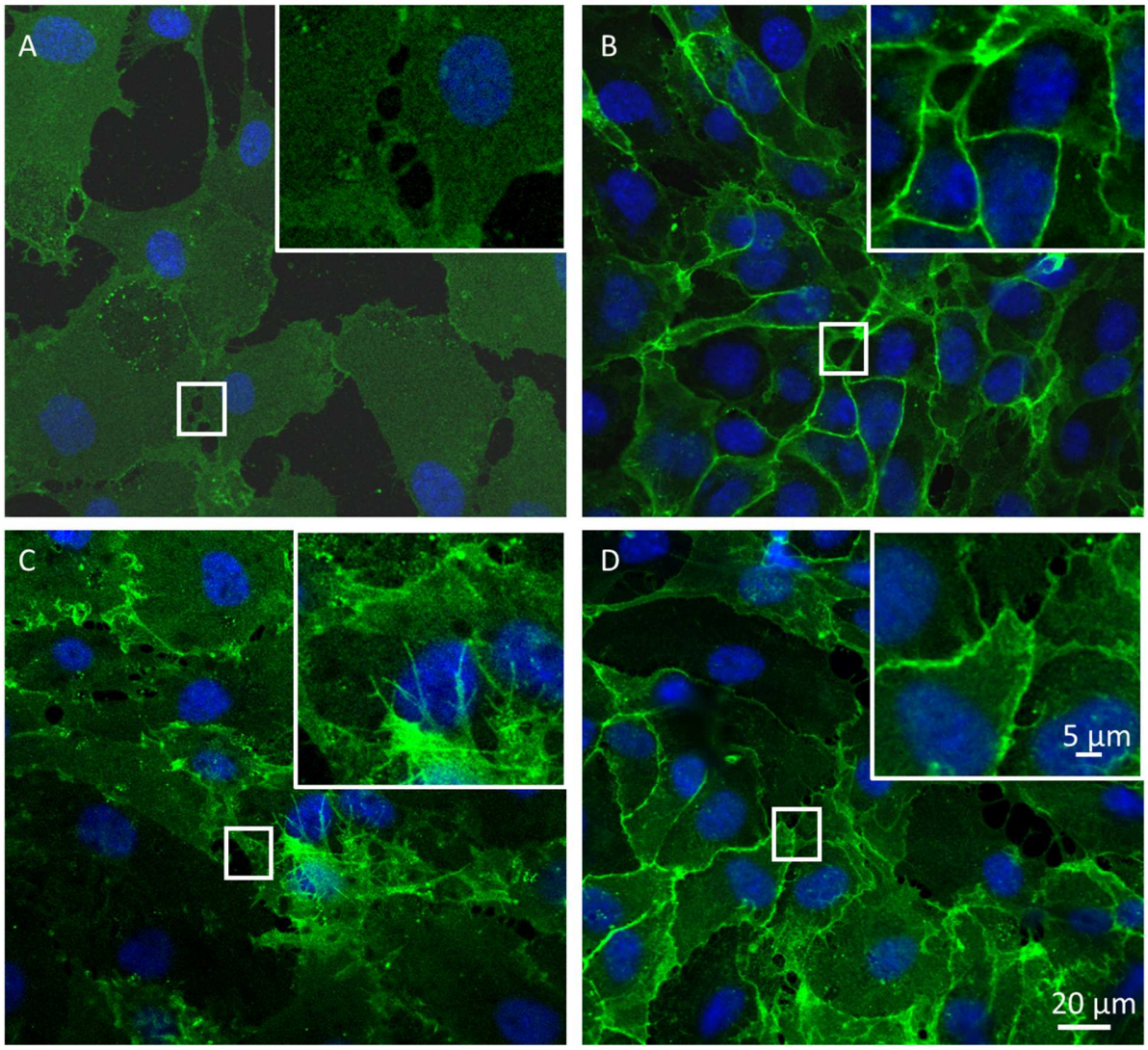

Figure 3. Confocal images with DAPI (blue) and PECAM-1 (green) staining after 7 days of HUVEC cells seeded on Gel (A), Gel + PAR (B), Gel/HA-Ald (C) and Gel/HA-Ald + PAR (D), with respectively digital zooms of cell-cell contact zones.

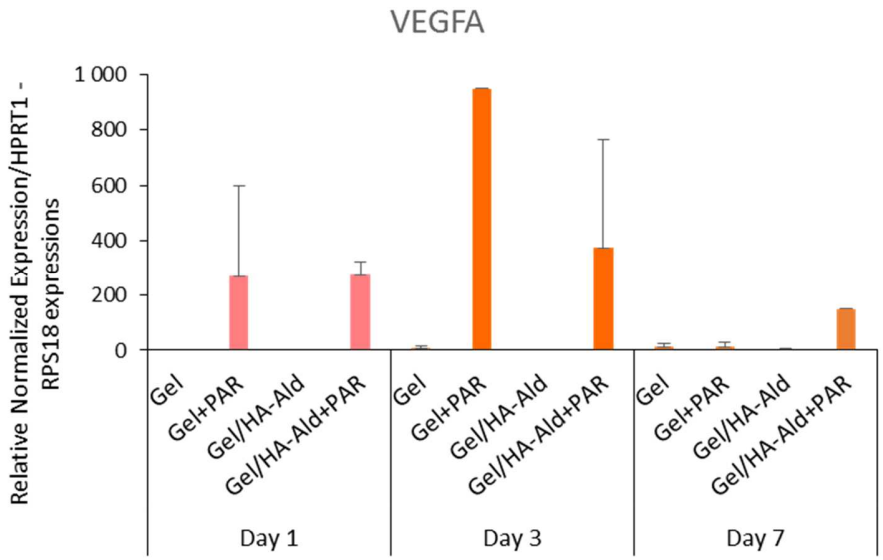

Figure 4. Q-PCR reading of vascular endothelial growth factor A (VEGFA) releasing from HUVEC cells.

Antibacterial properties

The next step was the analysis of the antibacterial properties of the coating. For this study, two different coating were used Gel and Gel/HA-Ald only or supplemented with 1.5 nmol PAR. Coating were tested again *S. aureus*, a strain particularly implicated in implant related infections. *S. aureus* were incubated on the four different coatings for 24 hours at 37°C and the normalized growth was estimated by monitoring the OD at 620 nm using glass substrate with antibiotics in the medium as positive control and glass without antibiotics in the medium as negative control. Without PAR loaded in the coating, no significant inhibition was observed for both Gel and Gel/HA-Ald coatings (Figure 5A). However, after the supplementation of 1.5 nmol of PAR, bacteria total growth inhibition was observed for both coatings (97 ± 4 % for Gel and 94 ± 6 % for Gel/HA-Ald coatings). These results were confirmed with time-lapse experiments performed on Gel/HA-Ald coating with and without PAR supplementation (Figure 5B, C). Gel/HA-Ald

without any PAR shows bacteria proliferation with time (Figure 5B). However, once supplemented with PAR, absolutely no bacteria were visible and moreover we observed black particles which settle corresponding to dead bacteria (Figure 5C). Bacteria proliferation area on the film surface was determined by image analysis and this evolution was plotted as a function of time (Figure 5D). Finally the antibacterial properties can be attributed to the presence PAR within the coating structure as previously demonstrated by studies from our group.[11, 12] In polyelectrolyte multilayer coatings based on PAR, we found that short length PAR polypeptide (30 residues) can kill bacteria through a contact-killing mechanism. The positively charged PAR chains can interact with the negatively charged bacterial membrane with the consequence of killing them.[11] As the previous parts demonstrated, Gel/HA-Ald films have a higher capacity to retain PAR, this might have resulted in the loss of antimicrobial activity due to the decreased mobility of PAR in the composite films; however antimicrobial tests demonstrates that PAR is still active as an antimicrobial agent in composite films.

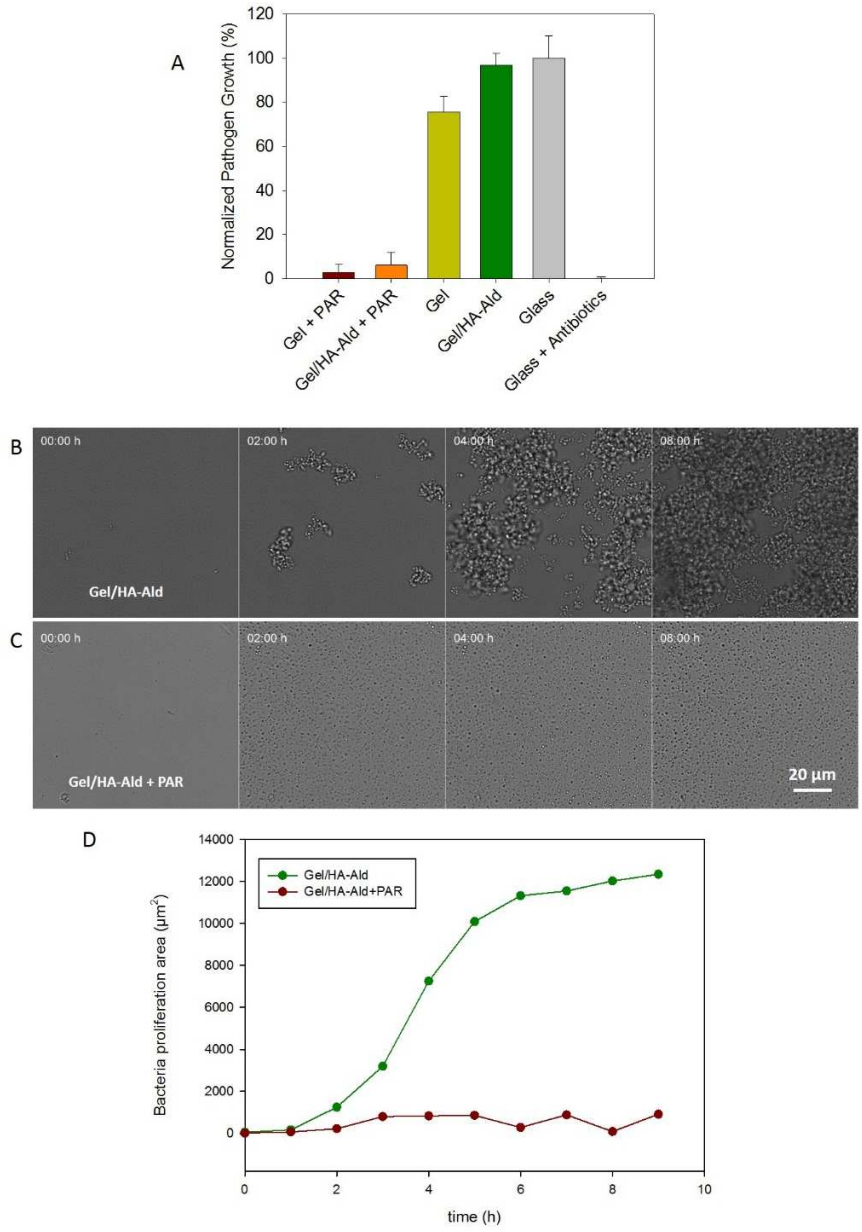

Figure 5. Antimicrobial bacterial test with 1.5 nmol supplementary PAR deposited on the films (A). Time lapse images of bacteria on Gel/HA-Ald (B) and on Gel/HA-Ald + PAR. Bacteria proliferation area in function of time for both films (D).

CONCLUSION

This work aimed to develop a new coating system which can retain significant amount of synthetic polypeptides such as poly(arginine) to provide multiple functions. Herein, we proposed a spin coated, interpenetrating network of gelatin and HA-Aldehyde derivative containing poly(arginine) in order to prevent the implant-related infections and also to promote implant integration via improved endothelial cell-cell contacts. The system harnesses the interactions between its components to achieve multiple biological functions inherent to the used bioactive molecules. This system easy to produce and can be used in future for coating of any kind of implantable device where there is a need for angiogenesis and a risk of infection.

ASSOCIATED CONTENT

Supporting Information is available Table S1 about PAR release experiment, Figure S1 about stability and mechanical properties of coatings and details note S1 about nanoplasmon sensing technique.

AUTHOR INFORMATION

* Corresponding authors: philippe.lavalle@inserm.fr and e.vrana@protipmedical.com

Author Contributions

The manuscript was written through contributions of all authors. All authors have given approval to the final version of the manuscript.

# These authors contributed equally.

Funding Sources

This project has received funding from the European Union's Seventh Framework Programme for research, technological development and demonstration under grant agreement no. 602694 (IMMODGEL), European Union's Horizon 2020 research and innovation programme under grant agreement no. 760921(PANBioRA) and FUI FASSIL.

ACKNOWLEDGMENT

We would like to thank Ms. Geraldine Koenig for RT-qPCR analysis, and Jenny Andersson from Insplorion for the PAR adsorption study.

REFERENCES

1. Ratner, B.; Horbett, T. *Biomaterials science: an introduction to materials in medicine. 2nd ed. San Diego: Elsevier* 2004, 237.
2. Schoen, F.; Anderson, J. *Biomaterials science: an introduction to materials in medicine. Elsevier, San Diego* 2004.
3. Morais, J. M.; Papadimitrakopoulos, F.; Burgess, D. J. *The AAPS journal* 2010**,** 12, (2), 188-196.
4. Edwards, R.; Harding, K. G. *Current opinion in infectious diseases* 2004**,** 17, (2), 91-96.
5. Buschmann, I.; Schaper, W. *News in physiological sciences : an international journal of physiology produced jointly by the International Union of Physiological Sciences and the American Physiological Society* 1999**,** 14, 121-125.
6. Risau, W. *Nature* 1997**,** 386, (6626), 671-674.
7. Schierholz, J. M.; Beuth, J. *Journal of Hospital Infection* 2001**,** 49, 87-93.
8. Foley, I.; Gilbert, P. *Biofouling* 1996**,** 10, 331-346.
9. Costerton, J. W.; Stewart, P. S.; Greenberg, E. P. *Science* 1999**,** 284, 1318-1322.
10. Campoccia, D.; Montanaro, L.; Arciola, C. R. *Biomaterials* 2006**,** 27, 2331-2339.
11. Mutschler, A.; Tallet, L.; Rabineau, M.; Dollinger, C.; Metz-Boutigue, M.-H.; Schneider, F.; Senger, B.; Vrana, N. E.; Schaaf, P.; Lavalle, P. *Chemistry of Materials* 2016**,** 28, (23), 8700–8709.
12. Mutschler, A.; Betscha, C.; Ball, V.; Senger, B.; Vrana, N. E.; Boulmedais, F.; Schroder, A.; Schaaf, P.; Lavalle, P. *Chemistry of Materials* 2017**,** 29, (7), 3195-3201.
13. Xie, L.; Song, X.; Tong, W.; Gao, C. *J. Colloid Interface Sci.* 2012**,** 385, (1), 274-281.
14. Knopf-Marques, H.; Pravda, M.; Wolfova, L.; Velebny, V.; Schaaf, P.; Vrana, N. E.; Lavalle, P. *Adv. Healthc. Mater.* 2016**,** 5, (18), 2841–2855
15. Burdick, J. A.; Prestwich, G. D. *Advanced materials* 2011**,** 23, (12), H41-H56.
16. Collins, M. N.; Birkinshaw, C. *Carbohydr. Polym.* 2013**,** 92, (2), 1262-1279.

17. Vercruysse, K. P.; Marecak, D. M.; Marecek, J. F.; Prestwich, G. D. *Bioconjugate Chem.* 1997**,** 8, (5), 686-694.
18. Bencherif, S. A.; Srinivasan, A.; Horkay, F.; Hollinger, J. O.; Matyjaszewski, K.; Washburn, N. R. *Biomaterials* 2008**,** 29, (12), 1739-1749.
19. Camci-Unal, G.; Cuttica, D.; Annabi, N.; Demarchi, D.; Khademhosseini, A. *Biomacromolecules* 2013**,** 14, (4), 1085-1092.
20. Chen, J. P.; Leu, Y. L.; Fang, C. L.; Chen, C. H.; Fang, J. Y. *J. Pharm. Sci.* 2011**,** 100, (2), 655-666.
21. Li, J.; Wu, F.; Zhang, K.; He, Z.; Zou, D.; Luo, X.; Fan, Y.; Yang, P.; Zhao, A.; Huang, N. *ACS applied materials & interfaces* 2017**,** 9, (36), 30343-30358.
22. Wu, F.; Li, J.; Zhang, K.; He, Z.; Yang, P.; Zou, D.; Huang, N. *ACS applied materials & interfaces* 2016**,** 8, (1), 109-121.
23. West, D.; Kumar, S. *The biology of hyaluronan* 1989**,** 143, 187-207.
24. Ciftci, S.; Barthes, J.; Lavalle, P.; Özçelik, H.; Debry, C.; Dupret-Bories, A.; Vrana, N. E. *Materials & Design* 2016**,** 95, 648-655.
25. Knopf-Marques, H.; Barthes, J.; Wolfova, L.; Vidal, B. r. r.; Koenig, G.; Bacharouche, J.; Francius, G. g.; Sadam, H.; Liivas, U.; Lavalle, P. *ACS Omega* 2017**,** 2, (3), 918-929.
26. Riabov, V.; Salazar, F.; Htwe, S. S.; Gudima, A.; Schmuttermaier, C.; Barthes, J.; Knopf-Marques, H.; Klüter, H.; Ghaemmaghami, A. M.; Vrana, N. E. *Acta Biomaterialia* 2017.
27. Barthes, J.; Vrana, N. E.; Özçelik, H.; Gahoual, R.; François, Y. N.; Bacharouche, J.; Francius, G.; Hemmerlé, J.; Metz-Boutigue, M.-H.; Schaaf, P.; Lavalle, P. *Biomaterials science* 2015**,** 3, (9), 1302-1311.
28. Mero, A.; Pasqualin, M.; Campisi, M.; Renier, D.; Pasut, G. *Carbohyd. Polym.* 2013**,** 92, (2), 2163-2170.
29. Buffa, R.; Kettou, S.; Pospisilova, L.; Berkova, M.; Velebny, V., Google Patents: 2010.
30. Buffa, R.; Kettou, S.; Pospisilova, L.; Huerta-Angeles, G.; Chladkova, D.; Velebny, V., Google Patents: 2010.
31. Vanderhooft, J. L.; Alcoutlabi, M.; Magda, J. J.; Prestwich, G. D. *Macromolecular bioscience* 2009**,** 9, (1), 20-28.
32. Knopf-Marques, H.; Singh, S.; Htwe, S. S.; Wolfova, L.; Buffa, R.; Bacharouche, J.; Francius, G.; Voegel, J.-C.; Schaaf, P.; Ghaemmaghami, A. M. *Biomacromolecules* 2016**,** 17, (6), 2189–2198.
33. Rath, M.; Müller, I.; Kropf, P.; Closs, E. I.; Munder, M. *Frontiers in immunology* 2014**,** 5.
34. Pipili-Synetos, E.; Sakkoula, E.; Maragoudakis, M. *British journal of pharmacology* 1993**,** 108, (4), 855-857.
35. Hubbell, J. A.; Thomas, S. N.; Swartz, M. A. *Nature* 2009**,** 462, (7272), 449-460.
36. Özçelik, H.; Vrana, N. E.; Gudima, A.; Riabov, V.; Gratchev, A.; Haikel, Y.; Metz-Boutigue, M. H.; Carradò, A.; Faerber, J.; Roland, T. *Advanced healthcare materials* 2015**,** 4, (13), 2026-2036.
37. Orlando, G. *Transplantation* 2017**,** 101, (2), 234-235.
38. Zadpoor, A., Multidisciplinary Digital Publishing Institute: 2015.
39. Courtial, E.-J.; Perrinet, C.; Colly, A.; Mariot, D.; Frances, J.-M.; Fulchiron, R.; Marquette, C. *Additive Manufacturing* 2019.
40. Reitmaier, S.; Shirazi-Adl, A.; Bashkuev, M.; Wilke, H.-J.; Gloria, A.; Schmidt, H. *Journal of the Royal Society Interface* 2012**,** 9, (73), 1869-1879.

41. Russo, T.; D'Amora, U.; Gloria, A.; Tunesi, M.; Sandri, M.; Rodilossi, S.; Albani, D.; Forloni, G.; Giordano, C.; Cigada, A. *Procedia Engineering* 2013**,** 59, 233-239.
42. Ford, M. C.; Bertram, J. P.; Hynes, S. R.; Michaud, M.; Li, Q.; Young, M.; Segal, S. S.; Madri, J. A.; Lavik, E. B. *Proceedings of the National Academy of Sciences of the United States of America* 2006**,** 103, (8), 2512-2517.
43. Pinter, E.; Mahooti, S.; Wang, Y.; Imhof, B. A.; Madri, J. A. *The American Journal of Pathology* 1999**,** 154, (5), 1367-1379.